Supplementary Materials for

ATRIP deficiency impairs the replication stress response and manifests as microcephaly primordial dwarfism and immunodeficiency.

Evi Duthoo[1,2,3]†, Elien Beyls[1,2,3]†, Lynn Backers[1,4,5]†, Thorkell Gudjónsson[6], Peiquan Huang[6], Leander Jonckheere[7,8], Sebastian Riemann[8,9], Bram Parton[4,5], Likun Du[10], Veronique Debacker[1,2], Marieke De Bruyne[4,5], Levi Hoste[11], Ans Baeyens[12], Anne Vral[12], Eva Van Braeckel[7,8], Jens Staal[13,14], Geert Mortier[15], Tessa Kerre[2,16], Qiang Pan-Hammarström[10], Claus Storgaard Sørensen[6], Filomeen Haerynck[1,2,17]‡*, Kathleen BM Claes[4,5]‡*, Simon J Tavernier[1,2,4,13,14]‡

Corresponding authors:

Filomeen Haerynck, Filomeen.Haerynck@UGent.be; Kathleen BM Claes, Kathleen.Claes@UGent.be

The file includes:

Case descriptions

Personally identifiable patient information was redacted in accordance with medRxiv requirements.

Supplementary Figures

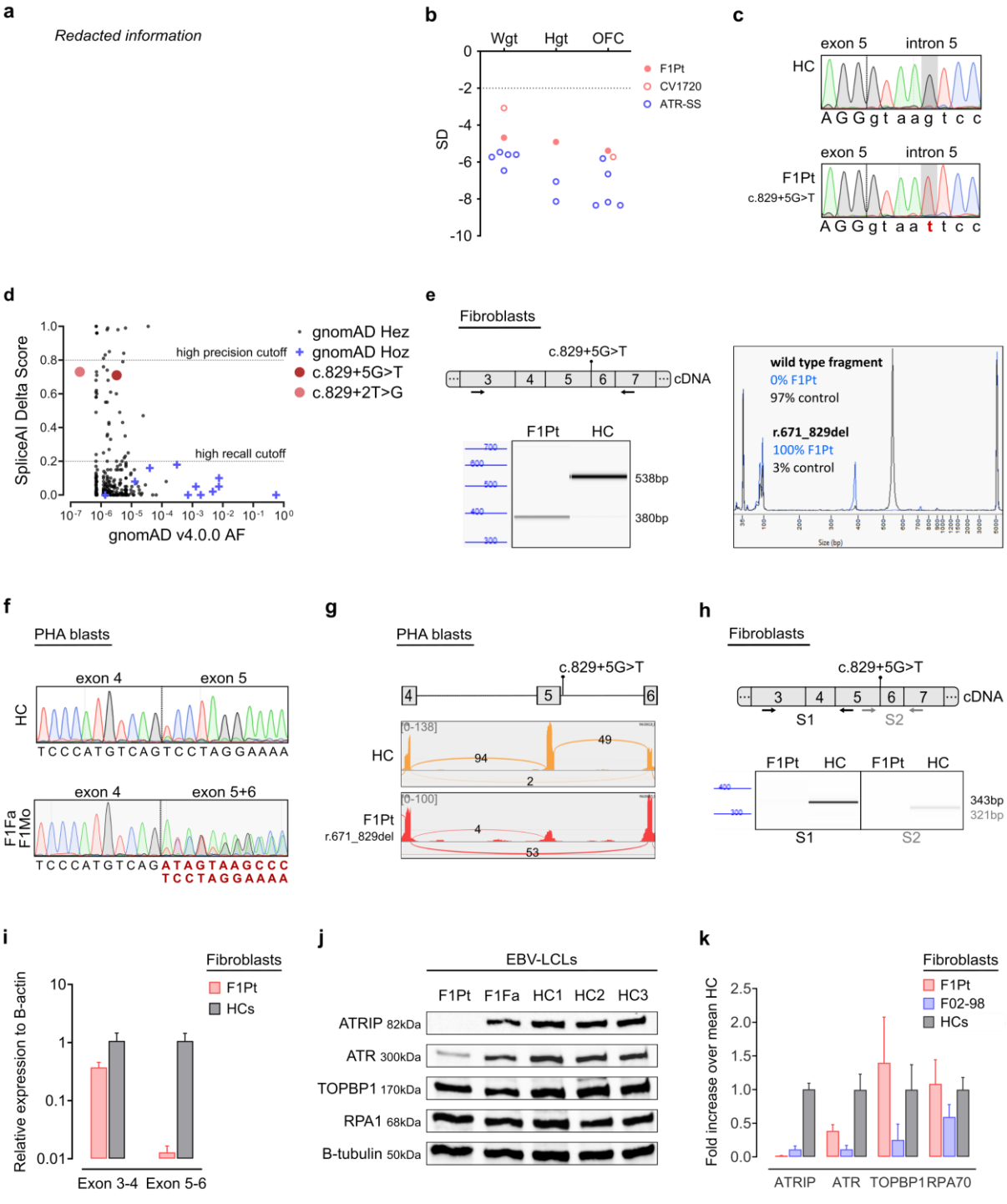

Supplementary Figure 1.

a Photographs of patients F1Pt and F46.1 demonstrating facial similarities, including sloping forehead and beak-like nose. **b** Weight (Wght), height (Hgt), and head circumference (occipital frontal circumference; OFC) at birth plotted as z-scores (SD from population mean for age and sex). Dashed line at -2SD indicates cut-off for normal population distribution. ATRIP patients are denoted by red dots, ATR patients are denoted by blue dots. **c** Electropherograms of genomic DNA extracted from blood for F1Pt and a healthy control (HC). Nucleotide numbering is in accordance with ENST00000320211.1. Images represent results from 5 independent experiments. **d** Population genetics: Highest SpliceAI Delta Score against gnomAD v4.0.0. allele frequency (AF) for splice region variants in *ATRIP* (ENST00000320211.1). Splice region variants are defined as nucleotide changes within

the ±20 base pairs (bp) flanking the exon. Black dots and blue cross signs represent heterozygous and homozygous variants, respectively. More details regarding homozygous splice variants can be found in Supplementary Table 4. Red shaded dots represent *ATRIP* variants of interest (c.829+5G>T and c.829+2T>G). **e** Fragment analysis and size profiles of PCR-amplified cDNA extracted from fibroblasts for F1Pt and a HC. Arrows indicate the position of forward and reverse primers used for PCR amplification. Percentages represent relative quantification of the 538bp wild type and 380bp mutant (r.7671_829del) fragment. Data are reflective of 2 independent experiments. **f** Electropherograms of cDNA extracted from PHA blasts for F1Fa (father), F1Mo (mother), and a HC. Nucleotide numbering is in accordance with ENST00000320211.1. Data are reflective of five independent experiments. **g** Sashimi plot of targeted RNA-seq data generated in Integrative Genomics Viewer (IGV). Input RNA was extracted from PHA blasts of F1Pt and a HC. Exon numbering is in accordance with ENST00000320211.1. **h** Fragment analysis of PCR-amplified cDNA using two primer pairs (S1: E3-E5; S2: E5-E7, indicated by arrows) on fibroblasts from F1Pt and a HC. Data is reflective of two independent experiments. **i** Real-time quantitative PCR (RT-qPCR) analysis on fibroblasts of F1Pt and HCs (n = 3) of amplicon in exon 3-4 and exon 5-6. The relative expression to β-actin in a logarithmic scale is shown. Data from 2 independent experiments is shown. **j** Endogenous protein expression of ATRIP and interaction partners in EBV immortalized lymphoblastoid cell lines (EBV-LCLs) from F1Pt, F1Fa, and HCs (n = 3). B-tubulin was used as loading control. Western blot image is reflective of two independent experiments. **k** Quantification in arbitrary units of digitized chemiluminescent signals from Fig. 1E normalized to β-tubulin signal from the same lane. Graph depicts fold increase of normalized protein levels over the mean of HCs (n = 3) of 4 immunoblots. Source data are provided as a Source Data file.

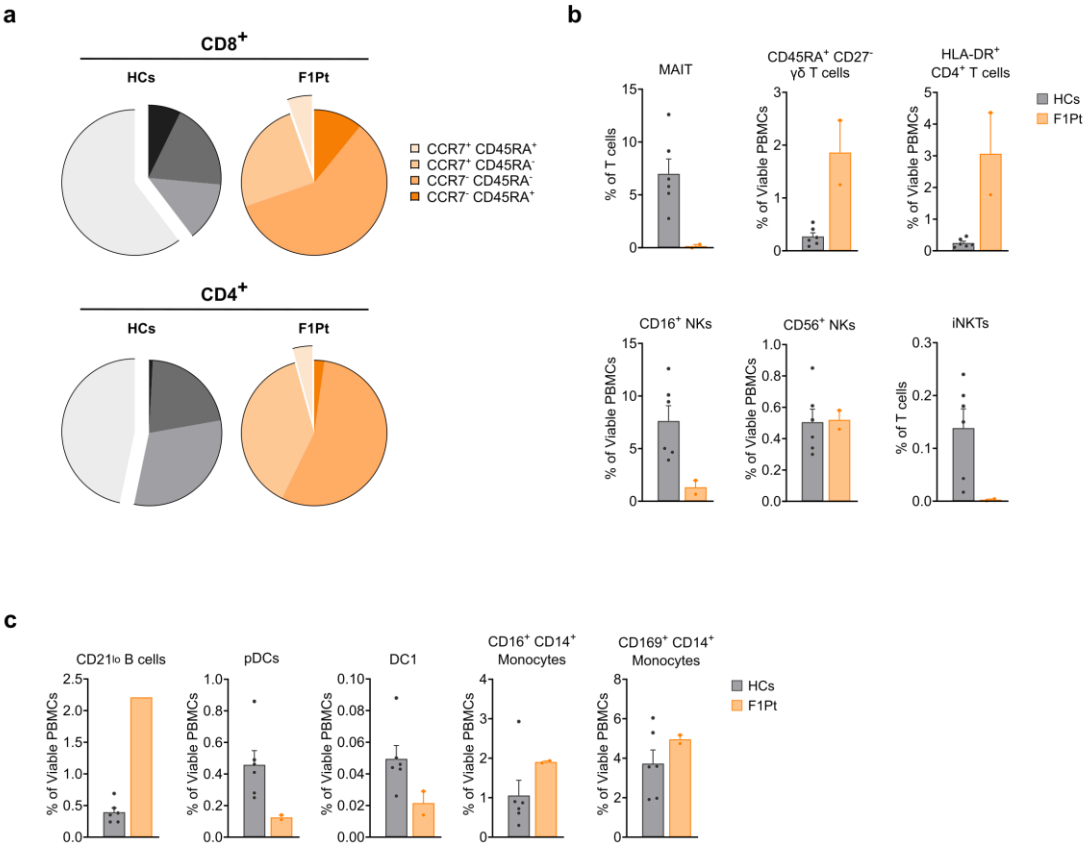

Supplementary Figure 2.

a Pie charts displaying the distribution of naïve T ($CCR7^+CD45RA^+$), T effector memory ($CCR7^-CD45RA^-$, T_{EM}), T central memory ($CCR7^+CD45RA^-$, T_{CM}), and terminally differentiated T effector ($CCR7^-CD45RA^+$, T_{EMRA}) cells in $CD8^+$ and $CD4^+$ T cells of ATRIP patient (F1Pt) and healthy controls (HCs) (n = 6). **b** Percentages of T and NK subsets in PBMCs of F1Pt and HCs (n = 6), based on manual gating of 25-parameter flow cytometry (FCM) data. Mean and SEM are shown. **c** Percentages of B and innate subsets in PBMCs of F1Pt and HCs (n = 6), based on manual gating of 25-parameter FCM data. Mean and SEM are shown.

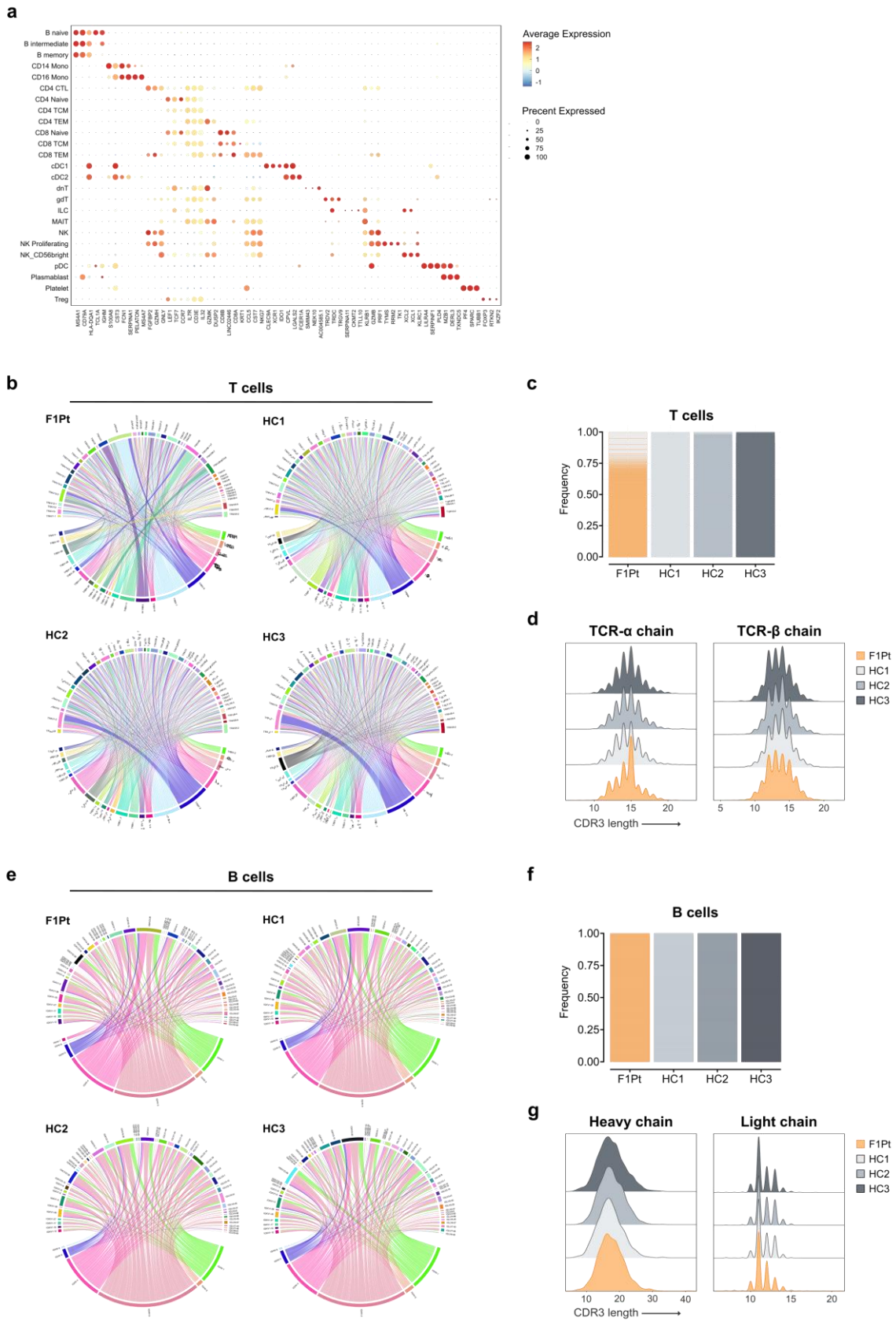

Supplementary Figure 3.

a Dotplot depicting signature genes defining the UMAP clusters shown in Fig. 3a. **b** Circos plots showing the *TRBV* and *TRAV* pairing pattern of T cells of ATRIP patient (F1Pt) and healthy controls (HCs). **c** Frequency of

unique T cell clones in F1Pt and HCs. **d** Distribution of the CDR3 region lengths of TCR-α and TCR-β clones of F1Pt and HCs T cells. **e** Circos plots demonstrating the *IGH*, *IGK*, and *IGK* pairing pattern of F1Pt and HCs B cells. **f** Frequency of unique B cell clones in F1Pt and HCs. **g** Distribution of the CDR3 region lengths of heavy and light chain of F1Pt and HCs B cells.

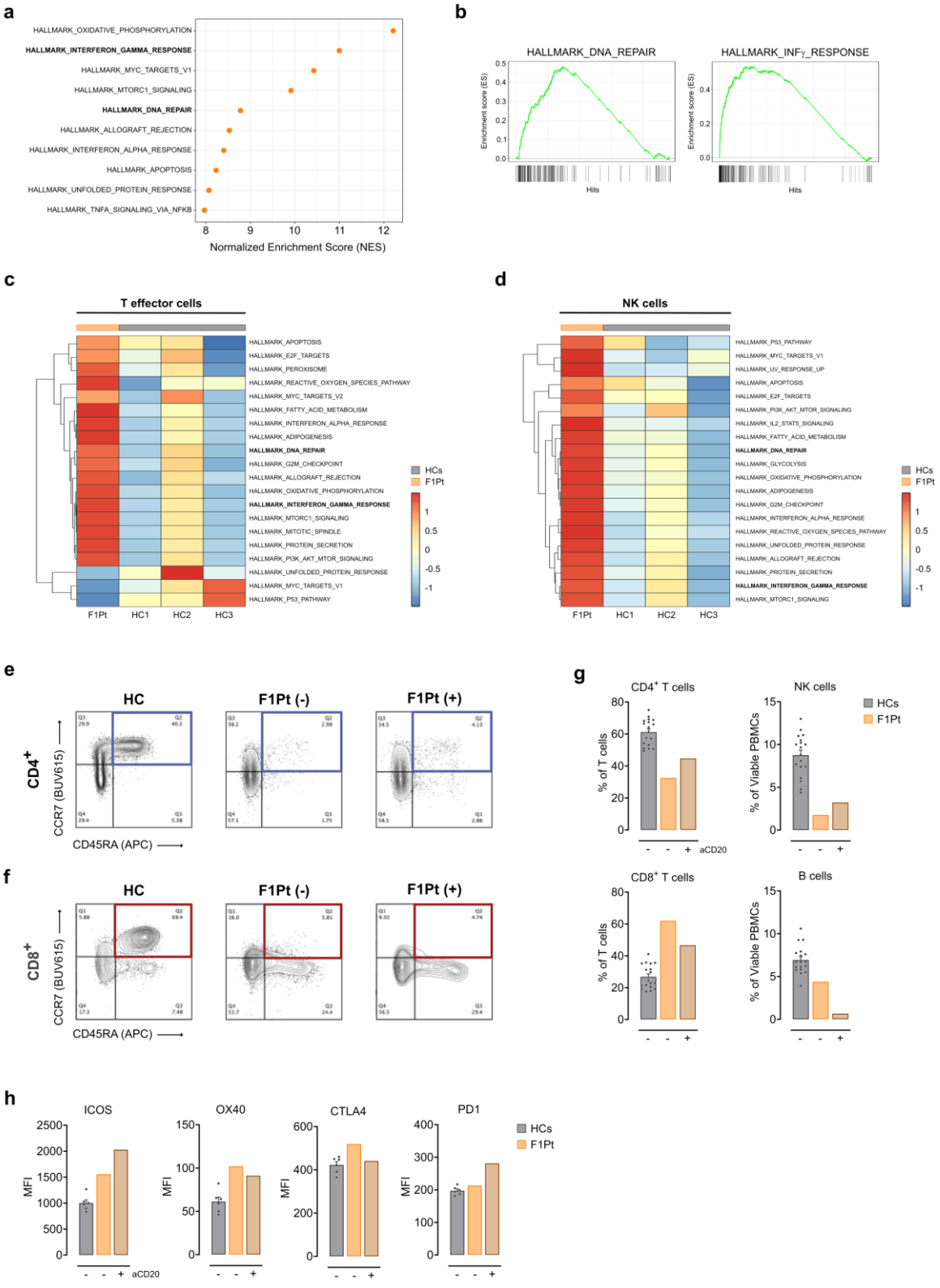

Supplementary Figure 4.

a MSigDB hallmark gene sets differentially expressed in PBMCs from F1Pt compared to HCs (n = 3). Normalized Enrichment Score (NES) values of the gene sets are depicted. **b** Enrichment plots for two MSigDB hallmark gene sets differentially expressed in PBMCs from F1Pt compared to HCs (n = 3). The profile of the running Enrichment Score (ES) is depicted for both hallmark gene sets. **c** Heatmap displaying the top 20 enriched hallmark gene sets (MSigDB) in T effector cells of F1Pt compared to HCs (n = 3). **d** Heatmap showing the top 20 enriched altered

hallmark gene sets (MSigDB) in NK cells of F1Pt compared to HCs (n = 3). **e** Contour plot showing $CD4^+$ T cell maturation in HC and F1Pt. F1Pt (-) represents pre-treatment with anti-CD20 mAb (aCD20), F1Pt (+) represents post-treatment with anti-CD20. **f** Contour plot displaying $CD8^+$ T cell maturation in HC and F1Pt. F1Pt (-) represents pre-treatment with anti-CD20, F1Pt (+) represents post-treatment with anti-CD20. **g** Frequencies of $CD4^+$ T, $CD8^+$ T, NK, and B cells in PBMCs from HCs (n = 18) and F1Pt pre- and post-treatment with anti-CD20. Data represents one experiment, with each datapoint representing one biological replicate. Mean and SEM are shown. **h** ICOS, OX40, PD1, and CTLA4 expression on $CD4^+$ T cells of HCs (n = 6) and F1Pt pre- and post-treatment with anti-CD20 mAb. Bar plots display median fluorescence (MFI). Mean and SEM are shown. Source data are provided as a Source Data file.

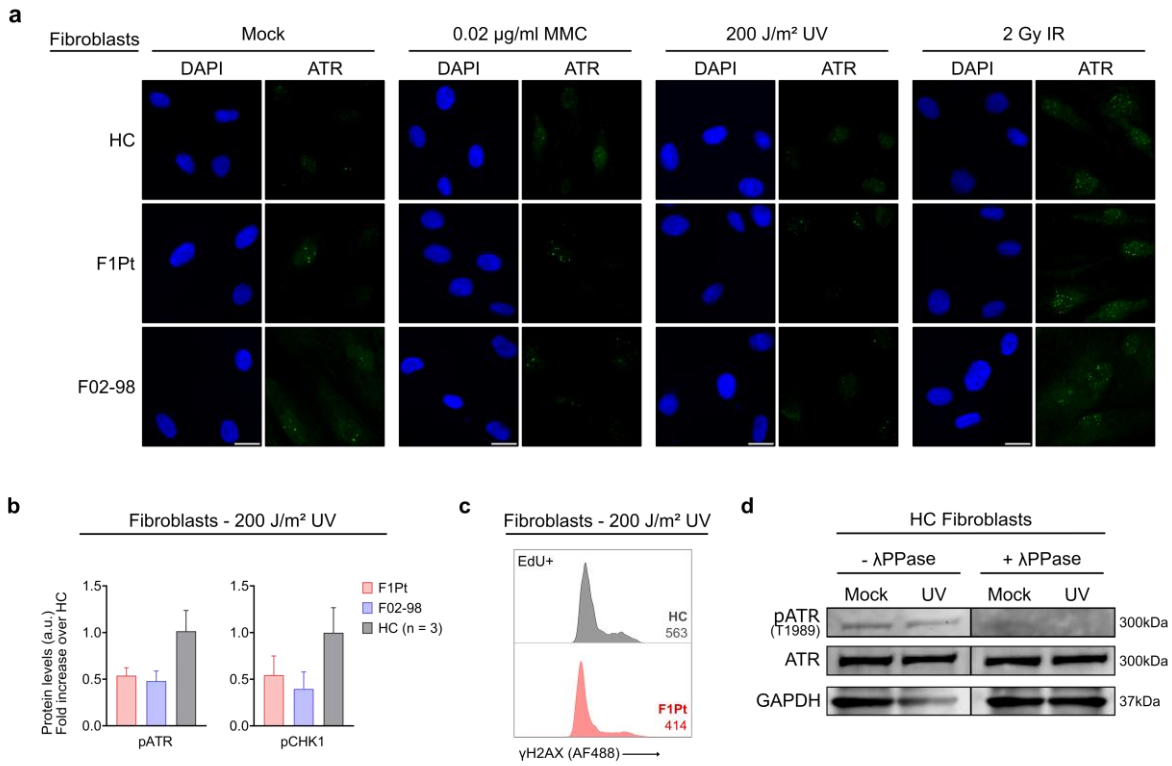

Supplementary Figure 5.

a Representative immunofluorescence images of cells shown in Fig. 2a with DAPI and ATR staining. Fibroblasts from a healthy control (HC), ATRIP patient (F1Pt), and ATR patient (F02-98) were left untreated or exposed to 0.02 µg/ml Mitomycin C (MMC), 200 J/m² UV or 2 Gy IR. ATR was stained by immunofluorescence following 24h (MMC) or 3h (UV and IR) of treatment. Images are representative of three independent experiments. Scale bars are 20 µm. **b** pATR and pCHK1 levels shown in Fig. 5b were quantified and represent three independent experiments. Bar graph depicts pATR and pCHK1 levels post 200 J/m² UV treatment, expressed as a fold increase over the mean levels observed in three healthy controls. Mean and SD are depicted. **c** γH2AX expression was determined by flow cytometric analysis 3h following 200 J/m² UV exposure in EdU+ fibroblasts of HC and F1Pt. Median fluorescence intensity (MFI) is annotated on the histogram. Data are reflective of one experiment. **d** Immunoblotting of T1989-pATR and total ATR with and without lambda phosphatase (λPPase) treatment on HC fibroblasts, untreated or 3h after 200 J/m² UV exposure. GAPDH serves as a loading control. Source data are provided as a Source Data file.

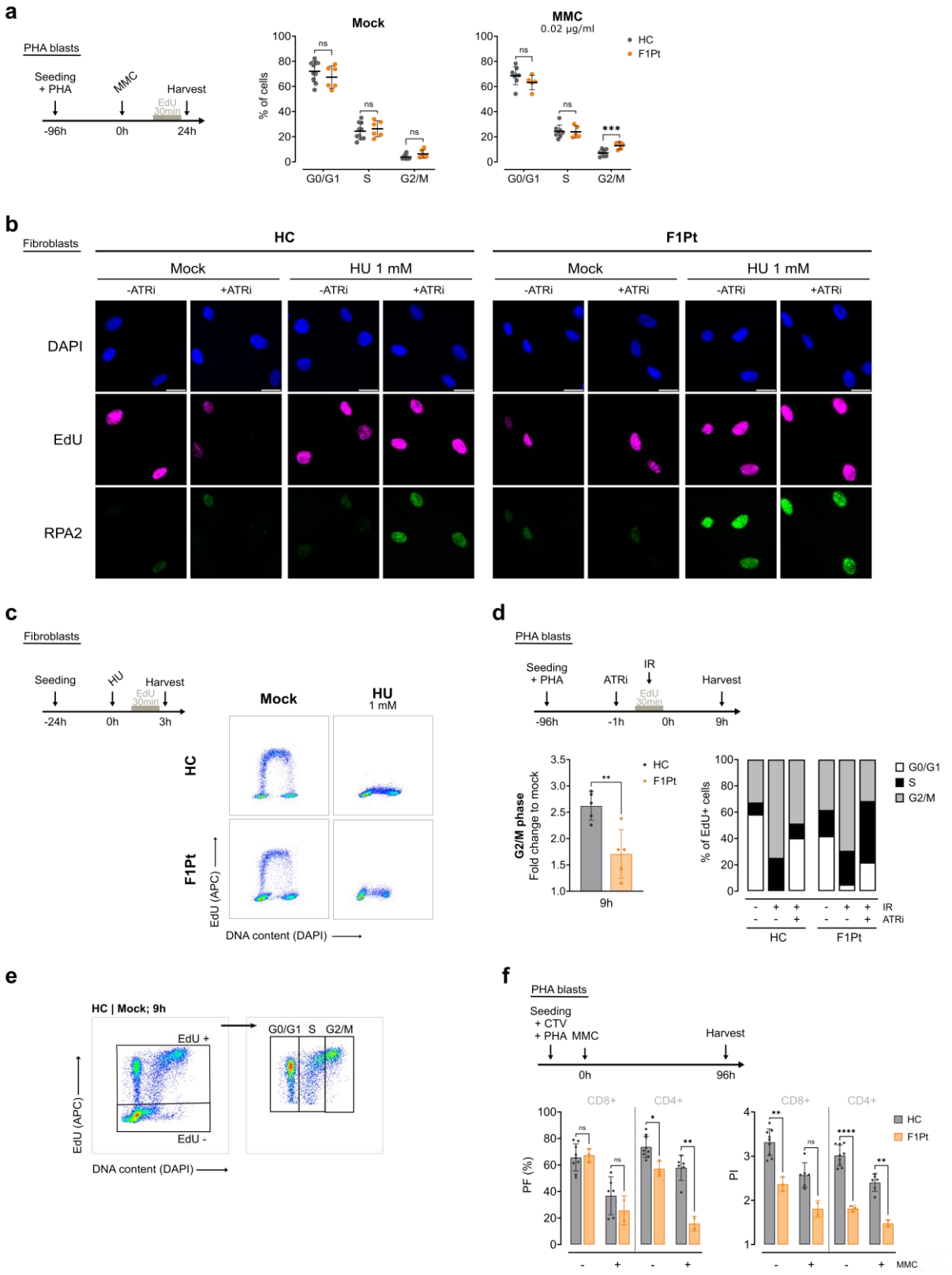

Supplementary Figure 6.

a Cell cycle distributions of PHA blasts from healthy controls (HCs) and ATRIP patient (F1Pt). Cells were either untreated or treated with 0.02 µg/ml Mitomycin C (MMC) and subsequently harvested at the timepoints indicated on the schematics. Scatter dot plot depicts data from at least five independent experiments. Mean and SD are shown. ns: not significant, *** p<0.001 (multiple paired t-tests). **b** Representative immunofluorescence images

with DAPI, EdU, and RPA staining of data shown in Fig. 6d. HC and F1Pt fibroblasts were untreated or exposed to 1 mM hydroxyurea (HU) for 3h. Images are representative of three independent experiments. Scale bars are 20 µm. **c** Flow cytometric (FCM) EdU pulse-labeling profiles of HC and F1Pt fibroblasts demonstrating the inhibiting effect of HU treatment on replication progression. Cells were exposed to 1 mM HU for 3h and subsequently harvested. Data are representative of two experiment. **d** EdU pulse-chase analysis after exposure to 4 Gy IR in the absence or presence of 20 nM ATRi. HC and F1Pt PHA blasts were harvested after 9h. Bar plot (left) shows EdU+ cells present in G2/M phase after IR exposure, depicted as a fold change over the percentage observed in the mock condition. Data represents 5 independent experiment. Mean and SD are shown. **p<0.01 (two-tailed paired t-test). Bar plot (right) shows percentages of EdU+ cells present in G0/G1, S, and G2/M phase. Data from one experiment is shown. **e** FCM gating strategy of EdU pulse-chase kinetics presented in Fig. 6g and Supplementary Fig. 6d. **f** Precursor frequency (PF) and proliferation index (PI) of $CD8^+$ and $CD4^+$ PHA blasts from HC and F1Pt. Cells were labeled with CellTrace Violet (CTV) and subsequently cultured for 96h in the presence or absence of 0.02 µg/ml MMC. Data of at least two independent experiment is shown, with each datapoint representing one biological replicate. Mean and SD are shown. ns: not significant, *p<0.05, **p<0.01, **** p<0.0001 (multiple paired t-tests). Source data are provided as a Source Data file.

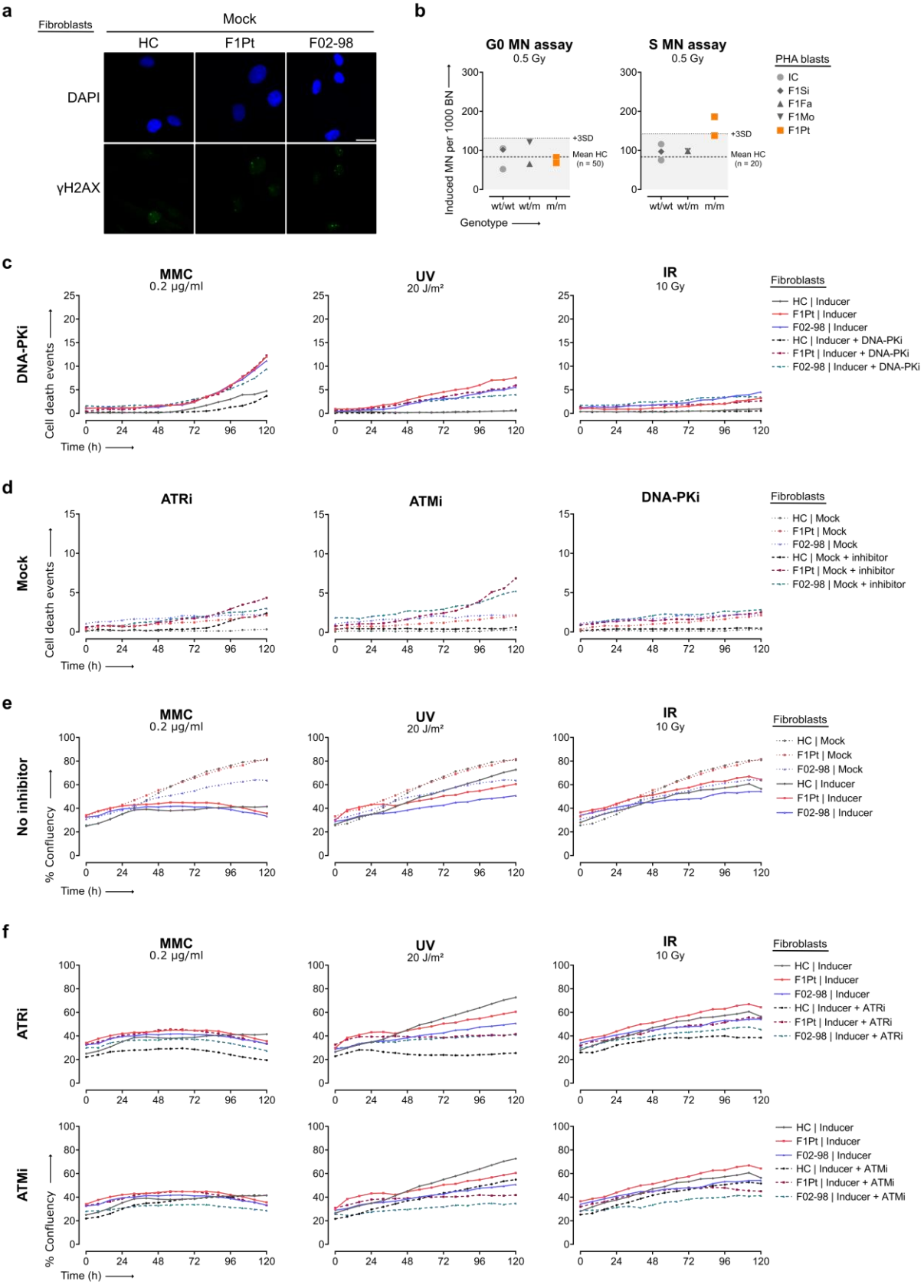

Supplementary Figure 7.

a Representative immunofluorescence images with DAPI and yH2AX staining of data shown in Fig. 7A. yH2AX foci are shown in untreated fibroblasts from a control (HC), ATRIP patient (F1Pt), and ATR patient (F02-98).

Images are representative of three independent experiments. Scale bars are 20 µm. **b** Using the G0 and S micronucleus (MN) assay, micronuclei were scored in PHA blasts exposed to 0.5 Gy ionizing radiation (IR). Mean MN values of a reference HC group are indicated by dashed lines. Dotted lines correspond to the mean of HCs + 3SD and serve as a cut-off for sensitivity to IR. Data of two independent experiments is shown for F1Pt, in each experiment an internal control (IC) was included. One experiment was performed for the family members (F1Si, F1Fa, F1Mo). **c, d** Fibroblasts from HC, F1Pt, and F02-98 were exposed to genotoxic inducers (0.2 µg/ml MMC, 20 J/m² UV, or 10 Gy IR) in combination with a specific kinase inhibitor (2 µM DNA-PKi) (**c**) or only treated with 20 nM ATRi, 10 µM ATMi, or 2 µM DNA-PKi (**d**). Cell death was monitored by live imaging up to 120h by quantifying the number of cells stained with SYTOX Green. Represented cell death kinetic plots are reflective of at least two independent experiments. **e, f** Corresponding proliferation curves of the data shown in Fig. 7g and h. Fibroblasts from HC, F1Pt, and F02-98 were untreated or exposed to genotoxic inducers (0.2 µg/ml MMC, 20 J/m² UV, or 10 Gy IR) without (**e**) or with (**f**) specific kinase inhibitors (20 nM ATRi or 10 µM ATMi) as indicated. Percentage of confluency was monitored by live imaging up to 120h. Data is representative of at least two independent experiments. Source data are provided as a Source Data file.

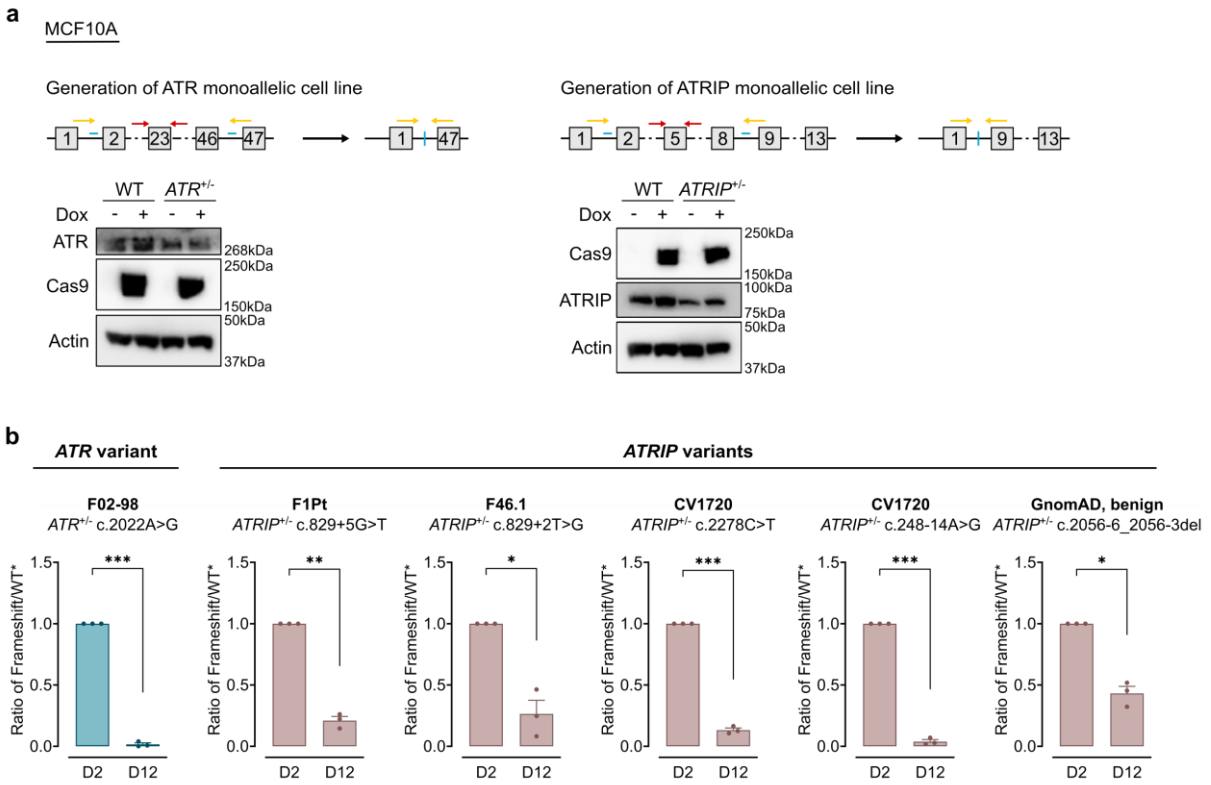

Supplementary Figure 8.

a Schematics of genome editing of the *ATR* and *ATRIP* allele (top). Blue lines represent the location of crRNAs, orange arrows depict the joint primers annealing to sequence outside the crRNA cutting regions, and red arrows represent the primers annealing to depletion region, used for WT allele detection. The western blot verification of mono-allelic cells is shown (bottom). Cells were seeded in 6 cm dish and 1 μg/ml doxycycline was added in the culture medium 24 hours before cell lysis to induce the expression of cas9 protein. **b** Cell fitness of MCF10A mono-allelic cells with frameshift mutations serving as internal control. Each variant has three independent biological replicates. Mean and SEM are shown. *p<0.05, **p<0.01, ***<0.001 (two-tailed paired t-tests). Source data are provided as a Source Data file.

Supplementary Tables

Supplementary Table 1. Clinical features of ATRIP patient (F1Pt). The clinical presentation is compatible with microcephaly primordial dwarfism (MPD).

Personally identifiable patient information was redacted in accordance with medRxiv requirements.

Supplementary Table 2. **Scores indicating aberrant splicing as predicted by various *in silico* tools (GRCh38, hg38).**

Prediction tool	g.48457421G>T, c.829+5G>T	g.48457418T>G, c.829+2T>G
SpliceAI Delta Score (donor loss)	0.71	0.73
Pangolin Delta Score (splice loss)	0.75	0.79
RF Score	0.874	0.926
ADA Score	0.99909	0.99997
MaxEntScan Difference	3.827	7.647
CADD/PHRED Score	23.5	33.0

Supplementary Table 3. Overview of homozygous *ATRIP* splice variants in gnomAD v4.0.0.

GnomAD variant ID (GRCh38)	rsID (dbSNP)	HGVS nomenclature (NM_130384.3)	Allele frequency (gnomAD v4.0.0)	Number of homozygotes (gnomAD v4.0.0)	SpliceAI Delta Score (effect, location)	ClinVar (Accession)	Pangolin Delta Score (effect, location)
3-48464565-A-C	rs2242150	c.1975-17A>C	0.560807635	256364	*0.01 (AG, -88bp)*	Not reported	0.01 (gain, 17bp)
3-48464823-T-C	rs3135937	c.2056-8T>C	0.007480602	552	0.10 (AG, 40bp)	Benign (VCV001267070.6)	0.02 (loss, 8bp)
3-48464819-C-A	rs3135936	c.2056-12C>A	0.007435878	549	0.05 (AG, 44bp)	Benign (VCV001276028.5)	0.03 (loss, 12bp)
3-48450188-T-C	rs11922041	c.381+18T>C	0.001880775	45	*0.00 (AL, -151bp)*	Benign (VCV001621536.5)	0.00 (loss, -18bp)
3-48450019-T-A	rs182766845	c.248-18T>A	0.004657135	26	0.02 (AG, 2bp) 0.02 (AL, 18bp)	Benign (VCV001613091.5)	0.11 (loss, 18bp)
3-48464149-C-T	rs138467436	c.1974+17C>T	0.000717299	11	0.00 (DL, -17bp) *0.04 (DG, 119bp)*	Benign (VCV001990326.1)	NA
3-48464815-A-AC	rs201468664	c.2056-9dup	0.001302093	2	0.05 (AG, 48bp)	Benign (VCV001987555.1)	0.04 (loss, 16bp)
3-48464678-C-T	NA	c.2055+16C>T	0.000001368	1	0.00 (DG, -16bp)	Not reported	0.00 (gain, -16bp)
3-48464821-CCTCT-C	rs754954019	c.2056-6_2056-3del	0.00031091	1	0.18 (AG, 46bp)	Likely benign (VCV002065669.1)	NA
3-48464822-CT-C	rs367546309	c.2056-8del	0.000039899	1	0.16 (AG, 41bp)	Likely benign (VCV000742744.4)	0.05 (loss, 1bp)
3-48465474-C-CT	rs765487326	c.2309-8dup	0.000013017	1	0.08 (AG, 15bp)	Not reported	0.02 (gain, 13bp)

AG: acceptor gain; AL: acceptor loss; DG: donor gain; DL: donor loss; NA: not available

Supplementary Table 4. **Considered alternative diagnoses and the associated genes for patient F1Pt.** No other (likely) pathogenic variants were identified in patient F1Pt using whole exome sequencing (WES) analyzing both SNVs and CNVs (MAF cut-off <0.02).

Disorder	Associated genes
Seckel syndrome	*ATR, RBBP8, CENPJ, CEP152, DNA2, TRAIP, CEP63, NIN, NSMCE2*
MOPD type I/III	*RNU4ATAC*
MOPD type II	*PCNT*
Meier-Gorlin syndrome	*ORC1, ORC4, ORC6, CDT1, CDC6, CDC45L, GMNN, MCM5*
Silver-Russell syndrome	*ICR1, IGF2, PLAG1, HMGA2*
3M syndrome	*CUL7, OBSL1, CCDC8*
Cornelia de Lange syndrome	*NIPBL, SMC1A, HDAC8, RAD21, SMC3, BRD4*
Bloom syndrome	*BLM*
Fanconi anemia	*MAD2L2, MAD2B, FANCV, UBE2T, HSPC150, FANCT, PHF9, FANCL, FANCD2, FANCD, FACD, FAD, FANCE, FACE, XRCC2, FANCU, SPGF50, POF17, XRCC9, FANCG, FANCC, FACC, FANCF, BRCA2, FANCD1, BROVCA2, GLM3, PNCA2, RAD51, RECA, MRMV2, FANCR, FANCI, KIAA1794 ,SLX4, BTBD12, MUS312, KIAA1784, KIAA1987, FANCP, ERCC4, XPF, FANCQ, XFEPS, PALB2, FANCN, PNCA3, BROVCA5, RFWD3, FANCW, FANCA, FACA, FA1, FA, FAA, BRCA1, PSCP, BROVCA1, PNCA4, FANCS, RAD51C, FANCO, BROVCA3, BRIP1, BACH1, FANCJ, FANCB, FAAP95, FAAP90, FLJ34064*

Supplementary Table 5. Sequences of primers used for variant confirmation (gDNA), splice analysis (cDNA), and real-time qPCR (mRNA) analysis.

Primer sequence (5' → 3')	Anneal site	Reference	Comment
Variant confirmation (gDNA)			
Forward: *M13*–CTGACAAAGAATGGTAGACATATAATAG Reverse: *M13*–ATTGCTGATCACAGAAATTGG	Exon 5 + intron 5	ENST00000320211, GRCh38/hg38 (*ATRIP)*	Note, 5' M13 tag to allow subsequent Sanger sequencing with universal M13 primers. Sequence of M13 forward and reverse tag is TGTAAAACGACGGCCAGT and CAGGAAACAGCTATGACC, respectively.
Splice analysis (cDNA)			
Forward: *M13*–AAGATCACATTTTCTTCTTGAGCA Reverse: *M13*–CTGGGATCAAAGGCTGCTT	Exon 3 Exon 7	ENST00000320211, GRCh38/hg38 (*ATRIP)*	-
Reverse: GTGGGGAAGGGACATGTTAG	Exon 5	ENST00000320211, GRCh38/hg38 (*ATRIP)*	Sanger sequencing primer
Forward: GGAAAAACCCTTCTGTGGTT	Exon 5		Sanger sequencing primer
Real-time qPCR analysis (mRNA)			
Hs.PT.58.46500972	Exon 3-4	NM_130384 (*ATRIP)*	Primer pair
Hs.PT.58.15253191	Exon 5-6		Primer pair
Housekeeping gene RT-qPCR (mRNA)			
Forward: CTGGAACGGTGAAGGTGACA Reverse: AAGGGACTTCTTGTAACAATGCA	*ACTB* *ACTB*	-	-

Supplementary Table 6. Detailed overview of the monoclonal antibodies used for immunophenotyping.

Antigen	Fluorochrome	Clone	Company
CD3	BUV395	UCHT1	BD
CD8	BUV496	RPA-T8	BD
CD278	BUV563	DX29	BD Optibuild
CCR7	BUV615	2-L1-A	BD
HLA-DR	BUV661	G46-6	BD
CD95	BUV737	563	BD Optibuild
CD4	BUV805	SK3	BD
CXCR3	BV421	G025H7	Biolegend
CXCR5	BV480	RF8B2	BD
CD16	BV570	3G8	Biolegend
CD152	BV605	BNI3	Biolegend
CD39	BV650	TU66	BD Horizon
CD25	BV711	BC96	Biolegend
CCR4	BV750	1G1	BD Optibuild
CD28	BV785	CD28.2	Biolegend
TCRg/d	FITC	B1	Biolegend
PD1	BB660-P	EH12.1	BD
CD56	BB790-P	NCAM16-2	BD
CD134	PerCP Cy5-5	ACT35	Biolegend
FoxP3	PE	206D	Biolegend
CCR6	PE-Dazzle594	G034E3	Biolegend
SA	PE-Cy5	206D	BD
CD27	PE-Cy7	O323	Biolegend
CD45RA	APC	HI100	Biolegend
Va7.2	AF700	3C10	Biolegend
CD161	APC-Fire750	HP-3G10	Biolegend
Va24Ja18	biotin	6B11	Thermofisher
CD24	BUV395	ML5	BD
CXCR3	BUV496	1C8	BD Optibuild
CCR7	BUV615	2-L1-A	BD
HLA-DR	BUV661	G46-6	BD
CD86	BUV737	2331 (FUN-1)	BD
CD3	BUV805	UCHT1	BD
CD1c	BV421	L161	Biolegend
CD185	BV480	RF8B2	BD
CD16	BV570	3G8	Biolegend
IgD	BV605	IA6-2	Biolegend
CD11c	BV650	3.9	Biolegend
CD25	BV711	BC96	Biolegend
CD14	BV750	63D3	Biolegend
CD20	BV785	2H7	Biolegend
PD1	BB660	EH12.1	BD Horizon
CD169	BB515	7-239	BD Horizon
CD123	BB630	7G3	BD Horizon
CD94	PerCP-Cy5-5	18D3	Biolegend
CD21	PE	Bu32	Biolegend
CD64	PE-Dazzle594	10.1	Biolegend
IgM	PE-Cy5	G20-127	BD
CD19	PE-Cy7	HIB19	Biolegend
CD141	AF647	M80	Biolegend
CD27	R718	M-T271	BD
CD38	APC-eFire750	HIT2	Biolegend

Supplementary Table 7. Designed CRISPR RNAs (crRNAs) and PCR primers for generating the mono-allelic cell lines used in CRISPR-SELECT^{TIME}.

Mono-allelic cell line	crRNAs	PCR Primers
ATR$^{+/-}$	crRNA1: CACCTCTTCAATACACAGGC crRNA2: ATCTTTAATAAGTCTTGTAC	Primer for detecting WT allele: Forward: TGAACCTCACTGTCTTTTCCTT Reverse: AGTTTTAGAGCTGTGAACATCCT Joint Primer: Forward: TGAAGATGTGACCTCCCTCG Reverse: AGGGTTAAGGATGACATGAAGGA
ATRIP$^{+/-}$	crRNA1: TTACTCTTGAGAGCAAAGCA crRNA2: TACAGCCCAATAATGAAACC	Primer for detecting WT allele: Forward: TTGAGCTCAGCAGTTCCAGA Reverse: TCCAGTCCCTGCAGAGATTG Joint Primer: Forward: GAGGGTGAGGCACAAGA Reverse: GGGGAGCACGATGGACTGG

Supplementary Table 8. Designed CRISPR RNAs (crRNAs) and PCR primers for variants analysis with CRISPR-SELECT^{TIME}.

Variants	crRNAs	PCR Primers
ATR c.2022A>G	ATCCGGGCTAGTTGTGTTAG	Forward: ACACTCTTTCCCTACACGACGCTCTTCCGATCT TCCTTGAGTGGAGAACAGCAGT Reverse: TGACTGGAGTTCAGACGTGTGCTCTTCCGATCT ACCCTGCATACATAGCCAGACA
ATRIP c.829+5G>T	ATACATCAATAGATGACTAA	Forward: ACACTCTTTCCCTACACGACGCTCTTCCGATCT ACATGTCCCTTCCCCACCCCTG Reverse: TGACTGGAGTTCAGACGTGTGCTCTTCCGATCT TGTCCCCTCTGTGCCTTGTCAGA
ATRIP c.829+2T>G	ATACATCAATAGATGACTAA	Forward: ACACTCTTTCCCTACACGACGCTCTTCCGATCT ACATGTCCCTTCCCCACCCCTG Reverse: TGACTGGAGTTCAGACGTGTGCTCTTCCGATCT TGTCCCCTCTGTGCCTTGTCAGA
ATRIP c.2278C>T	GGGGTCAGCATGCTCATCCG	Forward: ACACTCTTTCCCTACACGACGCTCTTCCGATCT GCACGGCCTATCGCAGAAGGAC Reverse: TGACTGGAGTTCAGACGTGTGCTCTTCCGATCT ACCTCTGGAAGAAGCCATGGGGG
ATRIP c.248-14A>G	ATTTTTTACAGGTGATCATA	Forward: ACACTCTTTCCCTACACGACGCTCTTCCGATCT CTGCACTCCAACCTGGGTAACA Reverse: TGACTGGAGTTCAGACGTGTGCTCTTCCGATCT TGTGCCTGAAGTACCTCTAATTCGA
ATRIP c.2056-6_2056-3del	CGCTCTGACCACCTGAGAGA	Forward: ACACTCTTTCCCTACACGACGCTCTTCCGATCT AGGTGAGTGGGTAGGGGCCAAC Reverse: TGACTGGAGTTCAGACGTGTGCTCTTCCGATCT TCCGCACTGTCAGCCACTGTCT

Supplementary Table 9. Designed mutation (MUT) and wild-type (WT*) DNA repair templates for variants analysis with CRISPR-SELECT^{TIME}.

Variants	MUT repair template	WT* repair template
ATR c.2022A>G	CCTGCAGAGCTCCCATGAAGTAATCCGGGC TAGTTGTGTGAGTGGGTTTTTTATCTTATTGC AGCAGCAGAATTCTTGTAACAGAGTTCC	CCTGCAGAGCTCCCATGAAGTAATCCGGGC TAGTTGTGTGAGCGGATTTTTTATCTTATTGC AGCAGCAGAATTCTTGTAACAGAGTTCC
ATRIP c.829+5G>T	CAGACGGAGTCAGGATACAAGCCTCTGGTG GGCAGAGAGGGTAATTCCATTACTCATCTAT TGATGTATAACAAGCTACCCAAATATGTG	CAGACGGAGTCAGGATACAAGCCTCTGGTG GGCAGAGAAGGTAAGTCCATTACTCATCTAT TGATGTATAACAAGCTACCCAAATATGTG
ATRIP c.829+2T>G	TGCCAGACGGAGTCAGGATACAAGCCTCTG GTGGGCAGAGAGGGGAAGTCCATTACTCAT CTATTGATGTATAACAAGCTACCCAAATAT	TGCCAGACGGAGTCAGGATACAAGCCTCTG GTGGGCAGAGAAGGTAAGTCCATTACTCATC TATTGATGTATAACAAGCTACCCAAATAT
ATRIP c.2278C>T	TGCATCAGTTTGACCAGGTGATGCCGGGGG TCAGCATGCTCATTTGAGGGCTTCCTGATGT GACGGACTGTGAAGGTAAGCCTGCCAGAG	TGCATCAGTTTGACCAGGTGATGCCGGGGG TCAGCATGCTCATTCGTGGGCTTCCTGATGT GACGGACTGTGAAGGTAAGCCTGCCAGAG
ATRIP c.248-14A>G	TCTGGCAAAAGTGGGAAAATATTGGGTCCTG AAATGTATATGGAGCTATTTTTTACAGGTGAT CACAAGGTCCACAGATTATTAGATGGC	TCTGGCAAAAGTGGGAAAATATTGGGTCCTG AAATGTATATGGAACTATTTTTTACAGGTGAC CACAAGGTCCACAGATTATTAGATGGC
ATRIP c.2056-6_2056-3del	TAGGGTGCAGGCCATGGTGGCACCAGGCCT CAGTCTGCACCCCCCCTCAGGTGGTCAGAG CGCTCACGGTGATGTTGCACAGACAGTGGC	GTGCAGGCCATGGTGGCACCAGGCCTCAGT CTGCACCCCCCCTCTCTCAGGTCGTCAGAG CGCTCACGGTGATGTTGCACAGACAGTGGC